IEEE Control Systems Letters paper presented at
2023 62nd IEEE Conference on Decision and Control (CDC)
December 13-15, 2023. Marina Bay Sands, Singapore

Local convergence of multi-agent systems towards rigid lattices

Andrea Giusti[1], Marco Coraggio[2], and Mario di Bernardo[1,2]

***Abstract*— Geometric pattern formation is an important emergent behavior in many applications involving large-scale multi-agent systems, such as sensor networks deployment and collective transportation. Attraction/repulsion virtual forces are the most common control approach to achieve such behavior in a distributed and scalable manner. Nevertheless, for most existing solutions only numerical and/or experimental evidence of their convergence is available. Here, we revisit the problem of achieving pattern formation in spaces of any dimension, giving sufficient conditions to prove analytically that under the influence of appropriate virtual forces, a large-scale multi-agent swarming system locally converges towards a stable and robust rigid lattice configuration. Our theoretical results are complemented by exhaustive numerical simulations confirming their effectiveness and estimating the region of asymptotic stability of the rigid lattice configuration.**

I. Introduction

Many natural and artificial systems consist of multiple interacting agents; their behavior being determined by both the individual agent dynamics and their interaction. In some applications the number of *agents* can be extremely large (*large-scale multi-agent systems*) and the role played by their interconnections becomes predominant over their individual dynamics [1]. Examples include cell populations [2], swarming multi-robot systems [3], social networks [4] among many others. Some of the most relevant emerging behavior exhibited by these systems involve their *spatial organization, coordination*, and *cooperation* [5]. A notable case is *geometric pattern formation* [6] where the agents are required to self-organize into some desired *pattern*, such as, for example, triangular lattices consisting of repeating adjacent triangles. Applications of pattern formation include sensor networks deployment [7], collective transportation and construction [8], [9], and exploration and mapping [10].

Most of the existing distributed control algorithms for geometric pattern formation rely on the use of *virtual forces* (or *virtual potentials*), [7], [11]–[18]. Within this framework, agents move under the effect of forces generated by the presence of their neighboring agents and the environment, causing attraction, repulsion, alignment, etc.

This work was in part supported by the Research Project "SHARESPACE" funded by the European Union (EU HORIZON-CL4-2022-HUMAN-01-14. SHARESPACE. GA 101092889 - http://sharespace.eu), and by the Research Project "Centro Nazionale HPC, Big Data e Quantum Computing Italian Center for Super Computing (ICSC)", funded by European Union (PNRR CN00000013).

[1]Department of Electrical Engineering and Information Technology, University of Naples Federico II, Via Claudio 21, Naples, 80125, Italy.

[2]Scuola Superiore Meridionale, School for Advanced Studies, Largo S. Marcellino 10, Naples, 80138, Italy.

Contacts: mario.dibernardo@unina.it, andrea.giusti@unina.it, marco.coraggio@unina.it.

Interestingly, most strategies are validated only numerically or experimentally [7], [11]–[13]. Among the exceptions, in [19], a geometric control approach based on trigonometric functions is proposed to build triangular lattices, and its global convergence is proved. The extension to 3D spaces is validated analytically in [20]. Moreover, *harmonic approximation* [21] provides necessary conditions for the local stability of a lattice. These conditions are used in [14] to numerically design a virtual force that locally stabilizes a hexagonal lattice. A general analysis of the effects of attraction/repulsion virtual forces is carried out in [22], where the authors prove that the agents converge inside a bounded region, even though the specific equilibrium configuration is not characterized. We wish to remark here that formation control [15]–[17] differs from geometric pattern formation because of a typically smaller number of agents (order of tens) with, possibly, unique identifiers, numerous roles for the agents and often some coordinated motion of the agents. Similarly, when solving *flocking* control problems, the emergence of coordinated motion is the crucial concern [18], [23], [24].

In this paper, we revisit the problem of geometric pattern formation using *attraction/repulsion* virtual forces with the aim of bridging a gap in the existing literature and deriving a general proof of convergence when considering the formation of rigid lattice configurations. When compared to previous work, e.g. [18]–[22], our stability results (i) can be applied to most control laws based on virtual forces (or potentials), rather than only to a specific algorithm [19], (ii) are sufficient rather than necessary conditions, as, e.g., in [21], (iii) characterize the asymptotic configuration of the agents, rather than just proving its boundedness [22], and (iv) guarantee the emergence of rigid lattices rather than less regular ones, e.g., the α-lattices studied in [18], which allow for disconnected graphs and the coexistence of heterogeneous patterns (e.g., triangular and square).

II. Mathematical preliminaries

Given a vector $\mathbf{v} \in \mathbb{R}^d$, $[\mathbf{v}]_i$ is its i-th element, $\|\mathbf{v}\|$ its Euclidean norm, and $\hat{\mathbf{v}} \coloneqq \frac{\mathbf{v}}{\|\mathbf{v}\|}$ its direction. $\mathbf{0}$ denotes a column vector of appropriate dimension with all elements equal to 0. Given a matrix $\mathbf{A}$, $[\mathbf{A}]_{ij}$ is its (i,j)-th element.

Definition 1 (Incidence matrix): *Given a digraph with n vertices and m edges, its* incidence matrix $\mathbf{B} \in \mathbb{R}^{n\times m}$ *has elements defined as*

$$[\mathbf{B}]_{ij} \coloneqq \begin{cases} +1, & \text{if edge } j \text{ starts from vertex } i, \\ -1, & \text{if edge } j \text{ ends in vertex } i, \\ 0, & \text{otherwise.} \end{cases}$$

Copyright ©2023 IEEE

Definition 2 (Framework [16, p. 120]): *Consider a (di-)graph $\mathcal{G} = (\mathcal{V}, \mathcal{E})$ with n vertices, and a set of positions $\mathbf{p}_1, \dots, \mathbf{p}_n \in \mathbb{R}^d$ associated to its vertices, with $\mathbf{p}_i \neq \mathbf{p}_j \ \forall i, j \in \{1, \dots, n\}$. A* d-dimensional framework *is the pair $(\mathcal{G}, \bar{\mathbf{p}})$, where $\bar{\mathbf{p}} \coloneqq [\mathbf{p}_1^\mathsf{T} \ \cdots \ \mathbf{p}_n^\mathsf{T}]^\mathsf{T} \in \mathbb{R}^{dn}$. Moreover, the* length *of an edge, say $(i, j) \in \mathcal{E}$, is $\left\|\mathbf{p}_i - \mathbf{p}_j\right\|$.*

Definition 3 (Congruent frameworks [25, p. 3]): *Given a graph $\mathcal{G} = (\mathcal{V}, \mathcal{E})$ and two frameworks $(\mathcal{G}, \bar{\mathbf{p}})$ and $(\mathcal{G}, \bar{\mathbf{q}})$, these are* congruent *if $\left\|\mathbf{p}_i - \mathbf{p}_j\right\| = \left\|\mathbf{q}_i - \mathbf{q}_j\right\| \ \forall i, j \in \mathcal{V}$.*

Definition 4 (Rigidity matrix [25, p. 5]): *Given a d-dimensional framework with $n \geq 2$ vertices and m edges, its* rigidity matrix $\mathbf{M} \in \mathbb{R}^{m \times dn}$ *has elements defined as*

$$[\mathbf{M}]_{e,(jd-d+k)} \coloneqq \begin{cases} [\mathbf{p}_j - \mathbf{p}_i]_k, & \text{if edge } e \text{ starts from vertex } i \text{ and ends in vertex } j, \\ [\mathbf{p}_i - \mathbf{p}_j]_k, & \text{if edge } e \text{ starts from vertex } j \text{ and ends in vertex } i, \\ 0, & \text{otherwise.} \end{cases}$$

with $k \in \{1, \dots, d\}$.

Definition 5 (Infinitesimal rigidity [16, p. 122]): *A framework with rigidity matrix $\mathbf{M}$ is* infinitesimally rigid *if, for any infinitesimal motion, say $\mathbf{u}$,[1] of its vertices, such that the length of the edges is preserved, it holds that $\mathbf{M}\mathbf{u} = \mathbf{0}$.*

To give a geometrical intuition of the concept of infinitesimal rigidity, we note that an infinitesimally rigid framework is also rigid [16, p. 122], according to the definition below.[2]

Definition 6 (Rigidity [25, p. 3]): *A framework is* rigid *if every continuous motion of the vertices, that preserves the length of the edges, also preserves the distances between all pairs of vertices.*

Consequently, in a rigid framework, a continuous motion that does *not* preserve the distance between any two vertices also does *not* preserve the length of at least one edge.

Theorem 1 ([26, Theorem 2.2]): *A d-dimensional framework with $n \geq d$ vertices and rigidity matrix $\mathbf{M}$ is infinitesimally rigid if and only if* $\operatorname{rank}(\mathbf{M}) = dn - d(d+1)/2$.

We denote by *swarm* a set of $n \in \mathbb{N}_{>0}$ identical agents, say $\mathcal{S} \coloneqq \{1, 2, \dots, n\}$, that can move in $\mathbb{R}^d$ and interact with their neighbors to generate emergent behavior [5]. For each agent $i \in \mathcal{S}$, $\mathbf{x}_i(t) \in \mathbb{R}^d$ denotes its position at time $t \in \mathbb{R}_{\geq 0}$. Moreover, we call $\bar{\mathbf{x}}(t) \coloneqq [\mathbf{x}_1^\mathsf{T}(t) \ \cdots \ \mathbf{x}_n^\mathsf{T}(t)]^\mathsf{T} \in \mathbb{R}^{dn}$ the *configuration* of the swarm, define $\mathbf{x}_\mathrm{c}(t) \coloneqq \frac{1}{n}\sum_{i=1}^n \mathbf{x}_i(t) \in \mathbb{R}^d$ as its *center*, and denote by $\mathbf{r}_{ij}(t) \coloneqq \mathbf{x}_i(t) - \mathbf{x}_j(t) \in \mathbb{R}^d$ the relative position of agent i with respect to agent j.

Definition 7 (Adjacency set): *Given a swarm $\mathcal{S}$, the* adjacency set *of agent i at time t is $\mathcal{A}_i(t) \coloneqq \{j \in \mathcal{S} \setminus \{i\} : \|\mathbf{r}_{ij}(t)\| \leq R_\mathrm{a}\}$, where $R_\mathrm{a} \in \mathbb{R}_{>0}$ is the* maximum link length.

In practice, we will say that two agents are connected if and only if their distance is at most R_a; see Fig. 1a.

Definition 8 (Links): *A* link *is a pair $(i, j) \in \mathcal{S} \times \mathcal{S}$ such that $j \in \mathcal{A}_i(t)$; $\left\|\mathbf{r}_{ij}(t)\right\|$ is its* length. *The set of all links existing in a certain configuration $\bar{\mathbf{x}}$ is denoted by $\mathcal{E}(\bar{\mathbf{x}})$.*

Notice that $(i, j) \in \mathcal{E}(\bar{\mathbf{x}}) \Leftrightarrow (j, i) \in \mathcal{E}(\bar{\mathbf{x}})$.

[1] $\mathbf{u}$ can be interpreted as either a velocity or a small displacement.

[2] Rarely, a rigid framework is not infinitesimally rigid; e.g. [25, p. 7].

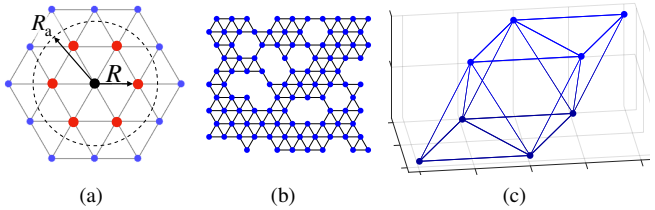

(a) (b) (c)

Fig. 1. (a) Adjacency set (red) of an agent (black). (b) A rigid lattice with $d = 2$, $n = 100$. (c) A rigid lattice with $d = 3$, $n = 8$.

Definition 9 (Swarm graph and framework): *The* swarm graph *is the digraph $\mathcal{G}(\bar{\mathbf{x}}) \coloneqq (\mathcal{S}, \mathcal{E}(\bar{\mathbf{x}}))$. The* swarm framework *is $\mathcal{F}(\bar{\mathbf{x}}) \coloneqq (\mathcal{G}(\bar{\mathbf{x}}), \bar{\mathbf{x}})$.*

Definition 10 (Rigid lattice): *Given a swarm with framework $\mathcal{F}(\bar{\mathbf{x}}^*)$, we call $\bar{\mathbf{x}}^*$ a* rigid lattice configuration *if*

(A) $\mathcal{F}(\bar{\mathbf{x}}^*)$ is infinitesimally rigid, and
(B) $\left\|\mathbf{r}_{ij}\right\| = R, \ \forall (i, j) \in \mathcal{E}(\bar{\mathbf{x}}^*)$,

where $R \in \mathbb{R}_{>0}$ denotes the desired link length.

Figs. 1b, 1c portray examples of rigid lattices, for $d = 2$ and $d = 3$: a tessellation of triangles, and one of tetrahedra and octahedra, respectively. It is immediate to verify that rigid lattices are characterized by connected graphs where each agent has at least d links, yielding robustness to link failure. A similar structure is the α-lattice from [18], which requires (B) but not (A) (hence, a rigid lattice is an α-lattice, but the converse is false). Thus, α-lattices can display more heterogeneous structures, containing different polytopes (e.g., squares, cubes), or even be disconnected, which can be unsuited for applications such as region coverage or distributed sensing. Note however that *vacancies*, i.e. holes in the lattice, can be present in both rigid and α-lattices.

In a rigid lattice, we denote by R_next the minimum distance between two not directly connected agents (e.g., $R_\mathrm{next} = R\sqrt{3}$ if $d = 2$ and $R_\mathrm{next} = R\sqrt{2}$ if $d = 3$). Here, we assume that $R_\mathrm{a} \in]R; R_\mathrm{next}[$, so that, when the swarm is in a rigid lattice configuration, the adjacency set (Definition 7) of any agent includes only the agents in its immediate surroundings, and all the links (Definition 8) have length R (see Fig. 1). Moreover, $\mathcal{T} \subset \mathbb{R}^{dn}$ is the set of all rigid lattice configurations; it is immediate to verify that $\mathcal{T}$ is unbounded and disconnected.

Definition 11 (Congruent configurations): *Given a configuration $\bar{\mathbf{x}}^\diamond$, we define* the set of its congruent configurations $\Gamma(\bar{\mathbf{x}}^\diamond)$ *as the set of configurations with congruent associated frameworks (see Definition 3), that is $\Gamma(\bar{\mathbf{x}}^\diamond) \coloneqq \{\bar{\mathbf{x}} \in \mathbb{R}^{dn} : \left\|\mathbf{x}_i - \mathbf{x}_j\right\| = \left\|\mathbf{x}_i^\diamond - \mathbf{x}_j^\diamond\right\|, \forall i, j \in \mathcal{S}\}$.*

These configurations are obtained by translations and rotations of the framework $\mathcal{F}(\bar{\mathbf{x}}^\diamond)$; thus, it is immediate to verify that $\Gamma(\bar{\mathbf{x}}^\diamond)$ is connected and unbounded for any $\bar{\mathbf{x}}^\diamond$ (see Fig. 2a). Also, note that $\bar{\mathbf{x}}^* \in \mathcal{T} \Leftrightarrow \Gamma(\bar{\mathbf{x}}^*) \subset \mathcal{T}$, and

$$\mathcal{T} = \bigcup_{\bar{\mathbf{x}}^* \in \mathcal{T}} \Gamma(\bar{\mathbf{x}}^*). \tag{1}$$

In the following, we omit the dependence on time when clear from the context.

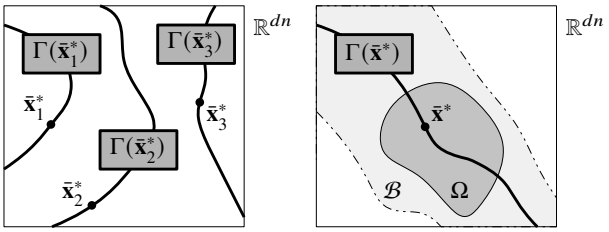

(a) (b)

Fig. 2. (a): Sets of rigid lattices configurations. (b): Sets used in the proof of Theorem 2.

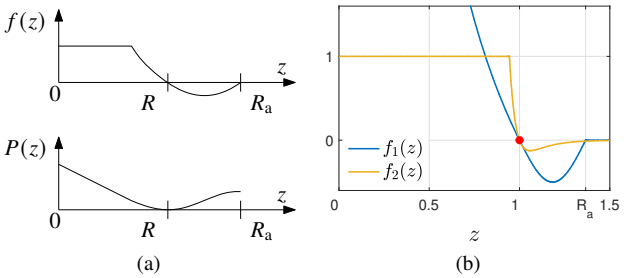

(a) (b)

Fig. 3. (a): An interaction function f satisfying Assumption 1 and its potential P. (b): Interaction functions in (12) and (13) in the case $d=2$. The red dot highlights the zero of the functions in $z=R$.

III. Problem Statement

Consider a swarm $\mathcal{S}$ of n agents, with agents' dynamics

$$\dot{\mathbf{x}}_i(t) = \mathbf{u}_i(t), \quad \forall i \in \mathcal{S}, \tag{2}$$

where $\mathbf{u}_i(t) \in \mathbb{R}^d$ is a distributed control law. We aim to select and validate such a law to let the swarm achieve a rigid lattice configuration. Then, let $R_s \in \mathbb{R}_{>0}$ be a *sensing radius* and define the *interaction set* of agent i at time t as

$$\mathcal{I}_i(t) \coloneqq \{j \in \mathcal{S} \setminus \{i\} : \|\mathbf{r}_{ij}(t)\| \leq R_s\}.$$

Given an *interaction function* $f : \mathbb{R}_{>0} \to \mathbb{R}$, we select $\mathbf{u}_i(t)$ in (2) as the distributed *virtual forces* control law

$$\mathbf{u}_i(t) \coloneqq \sum_{j \in \mathcal{I}_i(t)} f\left(\left\|\mathbf{r}_{ij}(t)\right\|\right) \hat{\mathbf{r}}_{ij}(t), \tag{3}$$

Note that in general there is no specific relation between $\mathcal{I}_i$ and $\mathcal{A}_i$ (see Definition 7); however, we reasonably assume that $R_s \geq R_a$, so that

$$\mathcal{A}_i \subseteq \mathcal{I}_i, \quad \forall i \in \mathcal{S}. \tag{4}$$

The following result slightly extends [22, Lemma 1].

Lemma 1: *The position of the center of the swarm, say* $\mathbf{x}_c$, *under the control law* (3) *is invariant, that is* $\dot{\mathbf{x}}_c = \mathbf{0}\ \forall \bar{\mathbf{x}} \in \mathbb{R}^{dn}$.

Proof. Exploiting (2) and (3), the dynamics of the center of the swarm is given by $\dot{\mathbf{x}}_c \coloneqq \frac{1}{n}\sum_{i=1}^n \dot{\mathbf{x}}_i = \frac{1}{n}\sum_{i=1}^n \mathbf{u}_i = \frac{1}{n}\sum_{i=1}^n \sum_{j\in\mathcal{I}_i} f\left(\left\|\mathbf{r}_{ij}\right\|\right)\hat{\mathbf{r}}_{ij}$. Since the existence of any link (i,j) implies the existence of link (j,i) (see Definition 7), for any term $f\left(\left\|\mathbf{r}_{ij}\right\|\right)\hat{\mathbf{r}}_{ij}$ there exists a term $f\left(\left\|\mathbf{r}_{ji}\right\|\right)\hat{\mathbf{r}}_{ji} = -f\left(\left\|\mathbf{r}_{ij}\right\|\right)\hat{\mathbf{r}}_{ij}$ (because $\left\|\mathbf{r}_{ij}\right\| = \left\|\mathbf{r}_{ji}\right\|$ and $\hat{\mathbf{r}}_{ij} = -\hat{\mathbf{r}}_{ji}$). Therefore, the sum of the two is zero, yielding the thesis. □

IV. Convergence to a rigid lattice configuration

We can now state our main result, i.e., that, given an interaction function f (in (3)) generating short range repulsion and long range attraction, the set of rigid lattice configurations is locally asymptotically stable ([27, Definition 1.8]).

Assumption 1: *f (in* (3)*) is such that:*

(a1) $f(R) = 0$,
(a2) $f(z) > 0$ *for* $z \in]0;R[$ *and* $f(z) < 0$ *for* $z \in]R;R_a[$,
(a3) $f(z)$ *is continuous in* $]0;R_a]$,
(a4) $f(z) = 0$ *for any* $z > R_a$.

An exemplary interaction function fulfilling the assumption above is portrayed in Fig. 3a.

Without loss of generality, we further assume that, under Assumption 1, in a sufficiently small neighborhood of a rigid lattice configuration, all other equilibria are also rigid lattice configurations (supporting evidence showing that this assumption is not restrictive is reported in the Appendix).

Theorem 2: *[Stability of rigid lattices] Let Assumption 1 hold. Then, for any rigid lattice configuration* $\bar{\mathbf{x}}^*$, $\Gamma(\bar{\mathbf{x}}^*)$ *is a locally asymptotically stable equilibrium set. Consequently,* $\mathcal{T}$ *is also a locally asymptotically stable equilibrium set.*

Proof. Let us consider *any* rigid lattice configuration $\bar{\mathbf{x}}^* \in \mathcal{T}$, with center $\mathbf{x}_c^* \coloneqq \frac{1}{n}\sum_{i=1}^n \mathbf{x}_i^*$ and relative positions $\mathbf{r}_{ij}^*$, and the set $\Gamma(\bar{\mathbf{x}}^*)$ of its congruent configurations. Recalling Definition 10.(B) and (a1), we have that $\bar{\mathbf{x}}^*$ is an equilibrium point of (2)–(3); thus, $\Gamma(\bar{\mathbf{x}}^*)$ and $\mathcal{T}$ are equilibrium sets. Next, we will prove local asymptotic stability of $\Gamma(\bar{\mathbf{x}}^*) \subset \mathcal{T}$, which implies local asymptotic stability of $\mathcal{T}$ through (1).

Step 1 (Lyapunov function): Given a configuration $\bar{\mathbf{x}} \in \mathbb{R}^{dn}$ with center $\mathbf{x}_c$ and inducing the links in $\mathcal{E}(\bar{\mathbf{x}})$ according to Definition 8, let $m \coloneqq |\mathcal{E}(\bar{\mathbf{x}})|$ and order the links in $\mathcal{E}(\bar{\mathbf{x}})$ arbitrarily, so that $\mathbf{r}_1, \ldots, \mathbf{r}_m$ refer to the relative positions $\mathbf{r}_{ij}$ for $(i,j) \in \mathcal{E}(\bar{\mathbf{x}})$. Recalling (a3), we can define the potential function $P :]0, R_a] \to \mathbb{R}$ given by $P(z) = -\int_R^z f(y)\,\mathrm{d}y$ (see Fig. 3a). Note that $P(R) = 0$, $\frac{\mathrm{d}P}{\mathrm{d}z}(z) = -f(z)$, and, from (a2),

$$P(z) > 0 \quad \forall z \in \mathbb{R}_{>0} \setminus \{R\}. \tag{5}$$

Then, let us consider the candidate Lyapunov function

$$V(\bar{\mathbf{x}}) \coloneqq \|\mathbf{x}_c^* - \mathbf{x}_c\|^2 + \sum_{k \in \mathcal{E}(\bar{\mathbf{x}})} P(\|\mathbf{r}_k\|). \tag{6}$$

By (5), it holds that $V(\bar{\mathbf{x}}) \geq 0\ \forall \bar{\mathbf{x}} \in \mathbb{R}^{dn}$, and $V = 0$ if and only if both $\mathbf{x}_c = \mathbf{x}_c^*$ and Definition 10.(B) holds.

Step 2 (Properties of V): $V(\bar{\mathbf{x}})$ is discontinuous over $\mathbb{R}^{dn}$ (because $\mathcal{E}(\bar{\mathbf{x}})$ changes when links (dis-)appear). However, $V(\bar{\mathbf{x}})$ is continuous and differentiable in any subset of $\mathbb{R}^{dn}$ where the set $\mathcal{E}(\bar{\mathbf{x}})$ of links is constant. To find such a set, we seek conditions on $\bar{\mathbf{x}}$ such that $\mathcal{E}(\bar{\mathbf{x}}) = \mathcal{E}(\bar{\mathbf{x}}^*)$ (see Definitions 7 and 8), i.e.,

$$\left\|\mathbf{r}_{ij}\right\| < R_a, \quad \forall (i,j) \in \mathcal{E}(\bar{\mathbf{x}}^*), \tag{7a}$$
$$\left\|\mathbf{r}_{ij}\right\| > R_a, \quad \forall (i,j) \notin \mathcal{E}(\bar{\mathbf{x}}^*). \tag{7b}$$

(7a) means that all links in $\mathcal{E}(\bar{\mathbf{x}}^*)$ are preserved in $\mathcal{E}(\bar{\mathbf{x}})$, while (7b) means that no new links are created in $\mathcal{E}(\bar{\mathbf{x}})$ with

respect to $\mathcal{E}(\bar{\mathbf{x}}^*)$. With simple algebraic manipulations it is possible to show that (7a) and (7b) hold if $\bar{\mathbf{x}} \in \mathcal{B}$, where

$$\mathcal{B} \coloneqq \{\bar{\mathbf{x}} \in \mathbb{R}^{dn} : \left|\left\|\mathbf{r}_{ij}\right\| - \left\|\mathbf{r}_{ij}^*\right\|\right| < \beta,\ \forall i,j \in \mathcal{S}\}, \quad (8)$$

and $\beta < \min_{i,j\in\mathcal{S}} \left|R_\mathrm{a} - \left\|\mathbf{r}_{ij}^*\right\|\right|$; $\mathcal{B}$ can be intended as a "neighborhood" of $\Gamma(\bar{\mathbf{x}}^*)$ with "width" β (see Fig. 2b). Thus, $\mathcal{E}(\bar{\mathbf{x}}) = \mathcal{E}(\bar{\mathbf{x}}^*)$ in $\mathcal{B}$ and V is continuously differentiable in $\mathcal{B}$.

Step 3 (Analysis of $\dot{V}$): Now, we restrict our analysis to the set $\mathcal{B}$ to study the attractivity of $\Gamma(\bar{\mathbf{x}}^*)$. We start by studying the dynamics of the agents. From (2)–(3), we have $\dot{\mathbf{x}}_i = \sum_{j\in\mathcal{I}_i} f(\|\mathbf{r}_{ij}\|)\hat{\mathbf{r}}_{ij}$. Hypothesis (a4) and (4) imply that $\sum_{j\in\mathcal{I}_i} f(\left\|\mathbf{r}_{ij}\right\|)\hat{\mathbf{r}}_{ij} = \sum_{j\in\mathcal{A}_i} f(\left\|\mathbf{r}_{ij}\right\|)\hat{\mathbf{r}}_{ij}$. Hence, using the incidence matrix $\mathbf{B}$ (Definition 1) of the swarm graph, we get

$$\dot{\mathbf{x}}_i = \sum_{j\in\mathcal{A}_i} f(\|\mathbf{r}_{ij}\|)\hat{\mathbf{r}}_{ij} = \sum_{k=1}^{m} [\mathbf{B}]_{ik} f(\|\mathbf{r}_k\|)\hat{\mathbf{r}}_k. \quad (9)$$

Moreover we can write the dynamics of the relative positions along a link k as $\dot{\mathbf{r}}_k = \sum_{i=1}^n [\mathbf{B}]_{ik}\dot{\mathbf{x}}_i$. Therefore, exploiting (6), Lemma 1, and (9), we get

$$\begin{aligned}\dot{V}(\bar{\mathbf{x}}) &= \sum_{k=1}^{m} \frac{\partial V}{\partial \|\mathbf{r}_k\|}\ \frac{\partial \|\mathbf{r}_k\|}{\partial \mathbf{r}_k}\ \dot{\mathbf{r}}_k = \sum_{k=1}^{m} P'(\|\mathbf{r}_k\|)\ \hat{\mathbf{r}}_k^\mathsf{T} \sum_{i=1}^{n} [\mathbf{B}]_{ik}\dot{\mathbf{x}}_i \\ &= -\sum_{i=1}^{n}\sum_{k=1}^{m} f(\|\mathbf{r}_k\|)\ [\mathbf{B}^\mathsf{T}]_{ki}\ \hat{\mathbf{r}}_k^\mathsf{T}\dot{\mathbf{x}}_i = -\sum_{i=1}^{n} \dot{\mathbf{x}}_i^\mathsf{T}\dot{\mathbf{x}}_i = -\dot{\bar{\mathbf{x}}}^\mathsf{T}\dot{\bar{\mathbf{x}}} \le 0,\end{aligned} \quad (10)$$

where we also used that $P' = -f$ and that $\frac{\partial\|\mathbf{r}_k\|}{\partial \mathbf{r}_k} = \hat{\mathbf{r}}_k^\mathsf{T}$. We can hence conclude that $\dot{V}(\bar{\mathbf{x}}) = 0$ if and only if $\dot{\bar{\mathbf{x}}} = \mathbf{0}$, i.e., in correspondence of equilibrium configurations.

Choosing β in (8) small enough, we exclude the presence of equilibrium configurations not belonging to $\Gamma(\bar{\mathbf{x}}^*)$, and hence

$$\begin{cases}\dot{V}(\bar{\mathbf{x}}) = 0, & \text{if } \bar{\mathbf{x}} \in \Gamma(\bar{\mathbf{x}}^*),\\ \dot{V}(\bar{\mathbf{x}}) < 0, & \text{if } \bar{\mathbf{x}} \in \mathcal{B}\setminus\Gamma(\bar{\mathbf{x}}^*).\end{cases} \quad (11)$$

Step 4 (Applying LaSalle's invariance principle): To complete the proof, we define a forward invariant neighborhood of $\bar{\mathbf{x}}^*$ and then apply LaSalle's invariance principle. Given some $\omega \in \mathbb{R}_{>0}$, let Ω be the largest connected set containing $\bar{\mathbf{x}}^*$ such that $V(\bar{\mathbf{x}}) \le \omega\ \forall \bar{\mathbf{x}} \in \Omega$ (see Fig. 2b). In particular, we select ω small enough that $\Omega \subseteq \mathcal{B}$.[3] Since $V(\bar{\mathbf{x}}) \le \omega$ and $\dot{V}(\bar{\mathbf{x}}) \le 0$ for all $\bar{\mathbf{x}} \in \Omega$, then Ω is forward invariant. Moreover, Ω is closed, because V is continuous in Ω, and Ω is the inverse image of the closed set $[0,\omega]$. Ω is also bounded because (i) translations too far from $\bar{\mathbf{x}}^*$ cause V to increase beyond ω (see (6)), and (ii) $\Omega \subseteq \mathcal{B}$ implies that the deformations of the framework are bounded (see (8)).

As Ω is closed, bounded (thus compact) and forward invariant, we can apply LaSalle's invariance principle [28, Theorem 4.4], and noting that, in Ω, $\dot{V}(\bar{\mathbf{x}}) = 0$ if and only if $\bar{\mathbf{x}} \in \Gamma(\bar{\mathbf{x}}^*)$ (see (11)), we get that all the trajectories starting in Ω converge to $\Gamma(\bar{\mathbf{x}}^*) \cap \Omega$. This and the forward invariance of Ω imply that $\Gamma(\bar{\mathbf{x}}^*)$ is locally asymptotically stable, and so is $\mathcal{T}$ because of (1). □

[3] Such ω exists because $\mathcal{B}$ is a "neighborhood" of $\Gamma(\bar{\mathbf{x}}^*)$ (in the sense of (8)) and, by the rigidity of framework $\mathcal{F}(\bar{\mathbf{x}}^*)$ (Definition 6), any continuous motion of the vertices that changes the distance between any two vertices also changes the length of at least one link, causing V to increase.

Proposition 1: *[Collision avoidance] Let $P^0 \coloneqq \lim_{z\searrow 0} P(z)$. (i) No collisions between agents occur if $P^0 = \infty$. (ii) In a sufficiently small neighborhood of a rigid lattice configuration, no collisions occur if $\bar{\mathbf{x}}(0)$ is such that $\sum_{k\in\mathcal{E}(\bar{\mathbf{x}})} P(\|\mathbf{r}_k\|) < P^0$.*

A proof of Proposition 1 can be found in the Appendix.

Remark 1: *[Path tracking] Path tracking can be obtained by adding a velocity term $\mathbf{w}(t)$ on the r.h.s. of (2). Theorem 2 still holds, as the analysis can be carried out on new states $\mathbf{y}_i$, with $\mathbf{y}_i(t) = \mathbf{x}_i(t) - \int_0^t \mathbf{w}(\tau)\mathrm{d}\tau$ and $\dot{\mathbf{y}}_i = \mathbf{u}_i$.*

Remark 1 only aims to show feasibility of path tracking; clearly, more sophisticated strategies can be designed.

Remark 2: *[Second order dynamics] It is possible to show that the results in Theorem 2 also hold in the case of second order nonlinear dynamics, that is $\dot{\mathbf{x}}_i = \mathbf{v}_i$, $\dot{\mathbf{v}}_i = g(\|\mathbf{v}_i\|)\hat{\mathbf{v}}_i + \mathbf{u}_i$, where $\mathbf{x}_i$ and $\mathbf{v}_i$ are the position and velocity of agent i, and $g : \mathbb{R}_{\ge 0} \to \mathbb{R}_{\le 0}$ is a friction term with $g(z) = 0 \Leftrightarrow z = 0$ and such that $\mathbf{v}_\mathrm{c}(t) \coloneqq \sum_{i=1}^n \mathbf{v}_i(t) \to \mathbf{0}$. Namely, the proof of Theorem 2 can be adapted by using the function $V = \sum_{k\in\mathcal{E}(\bar{\mathbf{x}})} P(\|\mathbf{r}_k\|) + \frac{1}{2}\sum_{i=1}^n \mathbf{v}_i^\mathsf{T}\mathbf{v}_i$ in (6) and exploiting that $\mathbf{x}_\mathrm{c}(t) \coloneqq \sum_{i=1}^n \mathbf{x}_i(t)$ remains bounded, to apply LaSalle's invariance principle.*

V. Numerical validation

In this section, we validate numerically the result presented in Section IV and estimate the basin of attraction of $\mathcal{T}$.

A. Simulation setup

We set $n = 100$, $R = 1$, $R_\mathrm{s} = 3$, $R_\mathrm{a} = (1 + R_\mathrm{next})/2$ (i.e. $R_\mathrm{a} \approx 1.37$ if $d = 2$; $R_\mathrm{a} \approx 1.21$ if $d = 3$). We validate our strategy using two interaction functions, depicted in Fig. 3b. The first one is

$$f_1(z) = \begin{cases} g\left(\frac{1}{z} - \frac{1}{R}\right)\frac{\pi R^2}{R_\mathrm{a} - R} & \text{if } z \in\ ]0;R],\\ -g\sin\left((z-R)\frac{\pi}{R_\mathrm{a}-R}\right) & \text{if } z \in\ ]R;R_\mathrm{a}],\\ 0 & \text{if } z > R_\mathrm{a};\end{cases} \quad (12)$$

with $g = 0.5$. f_1 satisfies Assumption 1, is smooth in $]0;R_\mathrm{a}[$ and $\lim_{z\searrow 0} f_1(z) = \infty$. The second interaction function f_2 is the Physics-inspired Lennard-Jones function [5], [11], i.e.,

$$f_2(z) = \min\left\{\left(\frac{a}{z^{2c}} - \frac{b}{z^c}\right),\ 1\right\}, \quad (13)$$

where we select $a = b = 0.5$ and $c = 12$ when $d = 2$ and $c = 24$ when $d = 3$; see Fig. 3b. f_2 saturates to 1 as $z \searrow 0$ to comply with possible actuator saturation. Moreover, f_2 satisfies (a1), (a2) and (a3) in Assumption 1 exactly, but (a4) only approximately. This is intentional as it allows to account for long range attraction between the agents, which is frequently required in swarm robotics applications [22].

To assess if the swarm is in a rigid lattice configuration, we check conditions (A), (B) in Definition 10. To evaluate (A) we use Theorem 1. To evaluate (B), we define the *error* $e(t) \coloneqq \max_{k\in\mathcal{E}(t)} |\|\mathbf{r}_k(t)\| - R|$, which is zero when (B) holds. Also, as long as $e(t)$ stays strictly lower than $R_\mathrm{a} - R$, links in the configuration of interest are neither created nor destroyed.

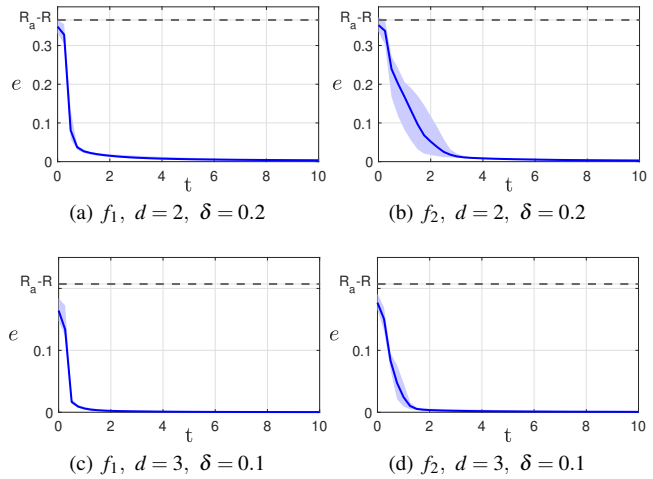

(a) f_1, $d=2$, $\delta=0.2$ (b) f_2, $d=2$, $\delta=0.2$

(c) f_1, $d=3$, $\delta=0.1$ (d) f_2, $d=3$, $\delta=0.1$

Fig. 4. Time evolution of e for various interaction functions and values of d. In each panel, 10 simulations with random initial conditions are showed; the solid line is the mean; the shaded area is the minimum and maximum.

For each simulation, the initial positions of the agents are obtained by picking a random rigid lattice configuration and then applying, to each agent, a different random displacement drawn from a uniform distribution over a disk (when $d=2$) or a sphere (when $d=3$), having radius $\delta \in \mathbb{R}_{\geq 0}$.

All simulation are run in MATLAB;[4] the agents' dynamics (2)–(3) are integrated using the forward Euler method with a fixed time step equal to 0.01 s.

B. Numerical results

To validate Theorem 2, in Fig. 4 we report the time evolution of the error $e(t)$ for 10 simulations where the swarm starts from a perturbed rigid lattice configuration. Simulations are presented for $d \in \{2,3\}$ and for both interaction functions f_1 and f_2. In all cases, infinitesimal rigidity is preserved and $e(t)$ converges to zero, denoting local stability of the lattice.

To estimate the basin of attraction of the set of rigid lattice configurations, we performed extensive simulations for various values of δ, and characterize the steady state configurations in Fig. 5. Namely, for δ smaller than 0.25 for $d=2$ and 0.2 for $d=3$ all simulations converge to a rigid lattice configuration. Then, as δ increases, fewer simulations converge to rigid lattices, until none does. Note that $e(0) \leq 2\delta$, therefore $\delta = 0.25$ (resp. $\delta = 0.2$) corresponds to a perturbation of up to 50% (resp. 40%) of the initial link length, giving an estimation of the basin of attraction of $\mathcal{T}$.

VI. Conclusions

We proved analytically local asymptotic stability of rigid lattices for swarms under the action of a distributed control law based on virtual attraction/repulsion forces. The theoretical derivations were supported by exhaustive numerical simulations, providing also an estimate of the basin of attraction.

[4]Simulations are performed using SwarmSim V2. The code is available at https://github.com/diBernardoGroup/SwarmSimPublic.

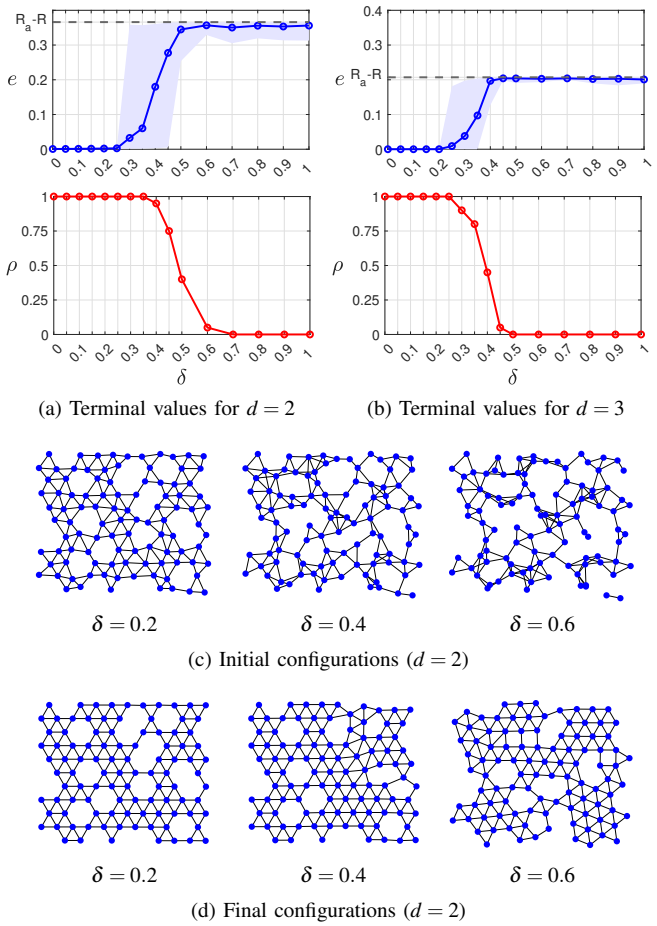

(a) Terminal values for $d=2$ (b) Terminal values for $d=3$

$\delta=0.2$ $\delta=0.4$ $\delta=0.6$

(c) Initial configurations ($d=2$)

$\delta=0.2$ $\delta=0.4$ $\delta=0.6$

(d) Final configurations ($d=2$)

Fig. 5. Simulations for different values of δ and interaction function f_2. (a), (b): Terminal values of e and ρ, respectively for $d=2$ and $d=3$. ρ is the fraction of simulations converging to an infinitesimally rigid configuration. For e, the solid line is the mean; the shaded area is the minimum and maximum. 20 simulations with random initial conditions are performed for each value of δ, and last 20 s. (c), (d): Initial and final configurations of representative simulations for specific values of δ in the case that $d=2$.

The mild hypotheses required on the interaction function allow for wide applicability of the theoretical results.

Future work will focus on an analytical characterization of the basin of attraction of $\mathcal{T}$, the study of the effect of measurement errors on the lattice configuration, anisotropic virtual forces, interaction with the environment (e.g. obstacle avoidance), and the extension of the results to other geometric lattices, such as squares and hexagons.

Appendix

To confirm the effectiveness of our theoretical results, we provide below further semi-analytical evidence that the set of rigid lattice configurations $\mathcal{T}$ is locally asymptotically stable, which also excludes the presence of other equilibria in an arbitrarily small neighborhood of it. To do so, we linearize system (2)–(3) around a rigid lattice configuration, say $\bar{\mathbf{x}}^*$, obtaining $\dot{\tilde{\mathbf{x}}} \approx \mathbf{J}(\bar{\mathbf{x}}^*)(\bar{\mathbf{x}} - \bar{\mathbf{x}}^*)$, with $\mathbf{J}(\bar{\mathbf{x}}^*) \in \mathbb{R}^{dn \times dn}$ derived as follows.

Jacobian of (2)–(3)*:* System (2)–(3) can be recast as

$$\dot{\bar{\mathbf{x}}} = ((\mathbf{B}\mathbf{F}\mathbf{G}^{-1}\mathbf{B}^{\mathsf{T}}) \otimes \mathbf{I}_d)\bar{\mathbf{x}} = ((\mathbf{B}\mathbf{H}\mathbf{B}^{\mathsf{T}}) \otimes \mathbf{I}_d)\bar{\mathbf{x}}, \tag{14}$$

where $\mathbf{F}, \mathbf{G}, \mathbf{H} \in \mathbb{R}^{m\times m}$ are diagonal matrices; $[\mathbf{F}]_{ii} \coloneqq f(\|\mathbf{r}_i\|)$, $[\mathbf{G}]_{ii} \coloneqq \|\mathbf{r}_i\|$, and $\mathbf{H} \coloneqq \mathbf{F}\mathbf{G}^{-1}$. The Jacobian of (14) is

$$\mathbf{J} = \left(\mathbf{B}\frac{\partial \mathbf{H}}{\partial \bar{\mathbf{x}}}\mathbf{B}^{\mathsf{T}} \otimes \mathbf{I}_d\right)\bar{\mathbf{x}} + (\mathbf{B}\mathbf{H}\mathbf{B}^{\mathsf{T}}) \otimes \mathbf{I}_d =: \mathbf{J}_1 + \mathbf{J}_2, \tag{15}$$

where $\frac{\partial \mathbf{H}}{\partial \bar{\mathbf{x}}} \in \mathbb{R}^{m\times m\times dn}$ is a tensor, and $\left[\frac{\partial \mathbf{H}}{\partial \bar{\mathbf{x}}}\mathbf{B}^{\mathsf{T}}\right]_{:,:,k} = \left[\frac{\partial \mathbf{H}}{\partial \bar{\mathbf{x}}}\right]_{:,:,k}\mathbf{B}^{\mathsf{T}} \in \mathbb{R}^{m\times n}$, with notation $[\,\cdot\,]_{:,:,k}$ denoting the matrix obtained by fixing the third index of the tensor. From (a1), for all rigid lattice configurations we have $\mathbf{J}_2 = (\mathbf{B}\mathbf{H}\mathbf{B}^{\mathsf{T}}) \otimes \mathbf{I}_d = \mathbf{0}$. Then, $[\mathbf{J}_1]_{:,k} = \left(\mathbf{B}\left[\frac{\partial \mathbf{H}}{\partial \bar{\mathbf{x}}}\right]_{:,:,k}\mathbf{B}^{\mathsf{T}} \otimes \mathbf{I}_d\right)\bar{\mathbf{x}}$. From [25, p. 20] we have $\frac{\partial \|\mathbf{r}_i\|^2}{\partial [\bar{\mathbf{x}}]_k} = 2[\mathbf{M}]_{i,k}$ (see Definition 4), that is $\frac{\partial \|\mathbf{r}_i\|}{\partial [\bar{\mathbf{x}}]_k} = \frac{1}{\|\mathbf{r}_i\|}[\mathbf{M}]_{i,k}$, and thus

$$\begin{aligned}\left[\frac{\partial \mathbf{H}}{\partial \bar{\mathbf{x}}}\right]_{i,i,k} &= \frac{\partial [f(\|\mathbf{r}_i\|)/\|\mathbf{r}_i\|]}{\partial \|\mathbf{r}_i\|}\frac{\partial \|\mathbf{r}_i\|}{\partial [\bar{\mathbf{x}}]_k} \\ &= [f'(\|\mathbf{r}_i\|)\|\mathbf{r}_i\| - f(\|\mathbf{r}_i\|)]\|\mathbf{r}_i\|^{-3}[\mathbf{M}]_{i,k}, \quad \text{(16a)}\\ \left[\frac{\partial \mathbf{H}}{\partial \bar{\mathbf{x}}}\right]_{i,j,k} &= 0, \quad \text{if } i \neq j. \quad \text{(16b)}\end{aligned}$$

Numerical analysis: We set $R = 1$ and generated 1520 random rigid lattice configurations (10 per each $n \in \{25, 26, \ldots, 100\}$, and each $d \in \{2, 3\}$). For each of these configurations, assuming f (in (3)) is in the form (13), we computed $\mathbf{J}$ using (15)–(16) and found that in all cases $\mathbf{J}$ has $d(d+1)/2$ zero eigenvalues with eigenvectors $\{\mathbf{w}_i^0\}_i$, and $dn - d(d+1)/2$ negative eigenvalues with eigenvectors $\{\mathbf{w}_j^{\pm}\}_j$. Moreover, $\mathbf{M}\mathbf{w}_i^0 = \mathbf{0}$ and $\mathbf{M}\mathbf{w}_j^{\pm} \neq \mathbf{0}$; thus, from Definition 5, the span of $\{\mathbf{w}_i^0\}$ corresponds to roto-translations and is a hyperplane locally tangent to $\Gamma(\bar{\mathbf{x}}^*)$ (see Definition 11), while $\{\mathbf{w}_j^{\pm}\}$ correspond to other motions. Therefore, the *center manifold theorem* [27, Theorem 5.1] yields that $\Gamma(\bar{\mathbf{x}}^*)$ is a *center manifold* of system (2)–(3). Moreover, as expected from Theorem 2, the *reduction principle* [27, Theorem 5.2] confirms that the dynamics locally converge onto the equilibrium set $\Gamma(\bar{\mathbf{x}}^*)$, and excludes the presence of other equilibria in an arbitrarily small neighborhood of it.

Proof of Proposition 1. When a collision occurs, at least one $\mathbf{r}_k$ becomes zero and thus, from (5), $\sum_{k\in\mathcal{E}(\bar{\mathbf{x}})} P(\|\mathbf{r}_k\|) \geq P^0$. Equations (6) and (10) yield the first statement. The second statement is obtained by recalling that $\Omega \subseteq \mathcal{B}$ and that Ω is forward invariant (see Step 4 of the proof of Theorem 2). □

REFERENCES

[1] P. Shi and B. Yan, "A survey on intelligent control for multiagent systems," *IEEE Transactions on Systems, Man, and Cybernetics: Systems*, vol. 51, no. 1, pp. 161–175, 2021.

[2] N. E. Grandel, K. Reyes Gamas, and M. R. Bennett, "Control of synthetic microbial consortia in time, space, and composition," *Trends in Microbiology*, vol. 29, no. 12, pp. 1095–1105, 2021.

[3] M. K. Heinrich, M. Wahby, M. Dorigo, and H. Hamann, "Swarm robotics," in *Cognitive Robotics*. The MIT Press, 2022, ch. 5, pp. 77–98.

[4] M. Jusup, P. Holme, K. Kanazawa, M. Takayasu, I. Romić, Z. Wang, S. Geček, T. Lipić, B. Podobnik, L. Wang, W. Luo, T. Klanjšček, J. Fan, S. Boccaletti, and M. Perc, "Social physics," *Physics Reports*, vol. 948, pp. 1–148, 2022.

[5] M. Brambilla, E. Ferrante, M. Birattari, and M. Dorigo, "Swarm robotics: a review from the swarm engineering perspective," *Swarm Intelligence*, vol. 7, no. 1, pp. 1–41, 2013.

[6] H. Oh, A. Ramezan Shirazi, C. Sun, and Y. Jin, "Bio-inspired self-organising multi-robot pattern formation: A review," *Robotics and Autonomous Systems*, vol. 91, pp. 83–100, 2017.

[7] H. Zhao, J. Wei, S. Huang, L. Zhou, and Q. Tang, "Regular topology formation based on artificial forces for distributed mobile robotic networks," *IEEE Transactions on Mobile Computing*, vol. 18, no. 10, pp. 2415–2429, 2019.

[8] M. Rubenstein, A. Cabrera, J. Werfel, G. Habibi, J. McLurkin, and R. Nagpal, "Collective transport of complex objects by simple robots," in *Proceedings of the 2013 International Conference on Autonomous Agents and Multi-agent Systems*, 2013, pp. 47–54.

[9] G. Gardi, S. Ceron, W. Wang, K. Petersen, and M. Sitti, "Microrobot collectives with reconfigurable morphologies, behaviors, and functions," *Nature Communications*, vol. 13, no. 1, pp. 1–14, 2022.

[10] M. Kegeleirs, G. Grisetti, and M. Birattari, "Swarm SLAM: Challenges and perspectives," *Frontiers in Robotics and AI*, vol. 8, no. March, pp. 1–6, 2021.

[11] A. Giusti, G. C. Maffettone, D. Fiore, M. Coraggio, and M. di Bernardo, "Distributed control for geometric pattern formation of large-scale multirobot systems," *arXiv:2207.14567 [cs.MA]*, 2022.

[12] W. M. Spears, D. F. Spears, J. C. Hamann, and R. Heil, "Distributed, physics-based control of swarms of vehicles," *Autonomous Robots*, vol. 17, no. 2-3, pp. 137–162, 2004.

[13] A. Casteigts, J. Albert, S. Chaumette, A. Nayak, and I. Stojmenovic, "Biconnecting a network of mobile robots using virtual angular forces," *Computer Communications*, vol. 35, no. 9, pp. 1038–1046, 2012.

[14] S. Torquato, "Inverse optimization techniques for targeted self-assembly," *Soft Matter*, vol. 5, no. 6, pp. 1157–1173, 2009.

[15] R. Olfati-Saber and R. M. Murray, "Distributed cooperative control of multiple vehicle formations using structural potential functions," *IFAC Proceedings Volumes*, vol. 35, no. 1, pp. 495–500, 2002.

[16] M. Mesbahi and M. Egerstedt, *Graph theoretic methods in multiagent networks*. Princeton University Press, 2010.

[17] K. Sakurama and T. Sugie, "Generalized Coordination of Multi-robot Systems," *Foundations and Trends in Systems and Control*, vol. 9, no. 1, pp. 1–170, 2021.

[18] R. Olfati-Saber, "Flocking for multi-agent dynamic systems: Algorithms and theory," *IEEE Transactions on Automatic Control*, vol. 51, no. 3, pp. 401–420, 2006.

[19] G. Lee and N. Y. Chong, "A geometric approach to deploying robot swarms," *Annals of Mathematics and Artificial Intelligence*, vol. 52, no. 2-4, pp. 257–280, 2008.

[20] G. Lee, Y. Nishimura, K. Tatara, and N. Y. Chong, "Three dimensional deployment of robot swarms," *IEEE/RSJ 2010 International Conference on Intelligent Robots and Systems*, pp. 5073–5078, 2010.

[21] K. Hinsen, "Normal mode theory and harmonic potential approximations," in *Normal Mode Analysis: Theory and Applications to Biological and Chemical Systems*, 2005, ch. 1, pp. 1–18.

[22] V. Gazi and K. M. Passino, "A class of attraction/repulsion functions for stable swarm aggregations," *Proceedings of the IEEE Conference on Decision and Control*, vol. 77, no. 18, pp. 2842–2847, 2002.

[23] F. Wang, G. Wang, and Y. Chen, "Adaptive spacing policy design of flocking control for multi-agent vehicular systems," *IFAC-PapersOnLine*, vol. 55, no. 37, pp. 524–529, 2022.

[24] G. Wang, M. Liu, F. Wang, and Y. Chen, "A Novel and Elliptical Lattice Design of Flocking Control for Multi-agent Ground Vehicles," *IEEE Control Systems Letters*, vol. 7, pp. 1159–1164, 2022.

[25] B. Jackson, "Notes on the Rigidity of Graphs," 2007. [Online]. Available: https://webspace.maths.qmul.ac.uk/b.jackson/levicoFINAL.pdf

[26] B. Hendrickson, "Conditions for unique graph realizations," *SIAM Journal on Computing*, vol. 21, no. 1, pp. 65–84, 1992.

[27] Y. A. Kuznetsov, *Elements of Applied Bifurcation Theory*, 2nd ed. Springer, 2004.

[28] H. K. Khalil, *Nonlinear Systems*, 3rd ed. Prentice Hall, 2002.